Structural and Magnetic Consequences of Protonation of the Oxo Bridge in Bis(hydridotripyrazolylborato)(μ-oxo)bis(μ-carboxylato)divanadium Complexes

Carl J. Carrano,* Ruben Verastgue, and Marcus R. Bond

Department of Chemistry, Southwest Texas State University, San Marcos, Texas 78666

Received February 25, 1993

Recently Wieghardt and co-workers have reported on the magnetic exchange interactions in homo/heteronuclear μ-(oxo)-bis(μ-carboxylato)dimetallic complexes and have provided a theoretical framework for understanding these effects.[1-4] Of the molecules studied, the divanadium complexes stand out for their deviation from the model presented by these authors. In particular, the divanadium complexes employing the 1,4,7-trimethyl-1,4,7-triazacyclononane capping ligand, TACN, show strong *ferromagnetic* (FM) exchange interactions in the oxo-bridged species which switch to *antiferromagnetic* (AFM) interactions upon protonation of the oxo bridge.[1] Unfortunately, these authors were unable to characterize the protonated complexes via X-ray diffraction, leaving unanswered questions about the structural changes accompanying protonation (and the resulting change in magnetic interactions). We have been studying vanadium complexes of the related hydridotripyrazolylborate ligand for some time and report here that we have been able to obtain crystal structures of both $[L_2V_2(\mu\text{-}O)(\mu\text{-}C_3H_5O_2)_2]$, **I**, and its protonated analog $[L_2V_2(\mu\text{-}OH)(\mu\text{-}C_3H_5O_2)]CF_3SO_3\cdot THF$, **II**, L = hydridotripyrazolylborate. Magnetic measurements confirm the switch from ferromagnetic to antiferromagnetic exchange upon protonation of these complexes. This data should lead to a better understanding of the magnetic properties and electronic structure in V(III) oxo-bridged dimers.

Synthesis of the oxo-bridged tripyrazolylborate species proceeded along similar lines to that of the analogous TACN complexes.[1] Recrystallization from acetonitrile gave deep green X-ray quality crystals. The structure of the oxo–propionate-bridged complex, **I**, is shown on the left in Figure 1.[5] While the differences between it and the corresponding TACN complex are minimal, there is however a general shortening of the bonds in the $HB(pz)_3$ species. This is most notable in the V–N bonds, which reflect the aromatic character of the pyrazolylborate nitrogens. Protonation of the deep green oxo–carboxylato-bridged complexes in acetonitrile by a variety of acids produces red/orange hydroxo–carboxylato-bridged cationic species. These can be crystallized by layering the solutions with either ether or THF and allowing them to stand at −20 °C for several days. The structure of the triflate salt of the hydroxo–propionate-bridged dimer **II** is shown on the right on Figure 1, while Table I contains a direct comparison of important metrical parameters between the protonated and unprotonated forms.[6] As expected the $V\text{–}O_{bridging}$ bond lengthens by some 0.16 Å upon protonation. Unexpectedly however, there is an accompanying decrease in the V–O–V angle (from 133 to 123°), which leads to a smaller than anticipated overall increase in the V···V distance of 0.14 Å.

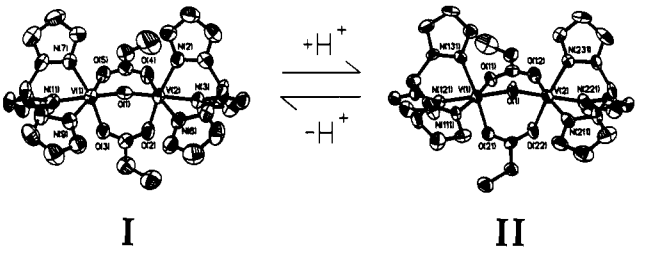

Figure 1. ORTEP diagram showing atom-labeling scheme for **I** (left) and its protonated analog, **II** (right). Important metrical parameters are given in Table I.

Table I. Comparison of Metrical Parameters between Protonated and Unprotonated $[L_2V_2(\mu\text{-}O)(\mu\text{-}C_3H_5O_2)_2]$

feature	protonated	unprotonated	Δ
$V\text{–}O_{oxo}$, Å	1.933	1.777	+0.16
V–O–V, deg	123.5	133.3	−9.9
V···V, Å	3.410	3.264	+0.146
$V\text{–}O_{propionate}$, Å	1.995	2.045	−0.061
$V\text{–}N_{trans}$, Å	2.095	2.183	−0.091
$V\text{–}N_{cis}$, Å	2.099	2.120	−0.029

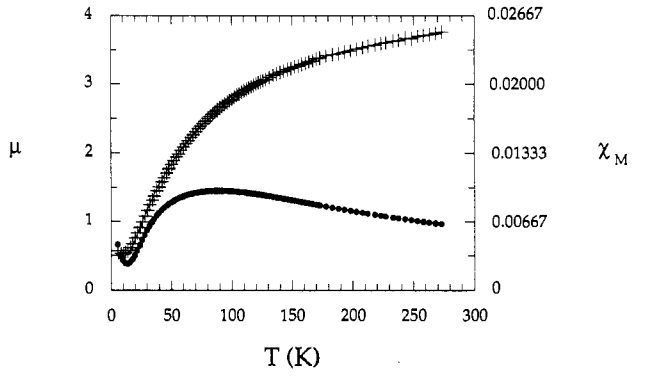

Figure 2. Plot of effective magnetic moment (left, crosses) and molar susceptibility per V_2 dimer (right, solid dots) for **II** as function of temperature.

Measurements of magnetic susceptibility vs. temperature over the range of ~5–280 K were performed on both **I** and **II**. Unprotonated **I** displays nearly ideal Curie–Weiss behavior, the value of μ being essentially independent of temperature. The value of the moment (μ_{eff} = 3.47(1) μ_B/V) is considerably higher than the spin only value for V(III) of 2.82 μ_B/V, suggesting strong ferromagnetic coupling to give an $S = 2$ ground state (μ_{eff} = 3.46 μ_B/V). Figure 2 shows a plot of both χ_m and μ_{eff} vs T for complex **II**. χ_m is seen to increase with decreasing temperature, reaching a maximum at ~75 K and declining thereafter until ~15 K

(1) Knopp, P.; Wieghardt, K. *Inorg. Chem.* **1991**, *30*, 4061.
(2) Hotzelmann, R.; Wieghardt, K.; Ensling, J.; Romstedt, H.; Gütlich, P.; Bill, E.; Flörke, U.; Haupt, H. J. *J. Am. Chem. Soc.* **1992**, *114*, 9470.
(3) Hotzelmann, R.; Wieghardt, K.; Flörke, U.; Haupt, H. J.; Weatherburn, D. C.; Bonvoisin, J.; Blondin, G.; Girerd, J. *J. Am. Chem. Soc.* **1992**, *114*, 1681.
(4) Hotzelmann, R.; Wieghardt, K. *Inorg. Chem.* **1993**, *32*, 114.
(5) Crystal data for I: $C_{32}H_{42}B_2N_{16}O_5V_2$, M = 854.3, monoclinic, $P2_1/n$, a = 13.406(3) Å, b = 15.313(3) Å, c = 22.217(4) Å, β = 106.75(3)°, V = 4367(2) Å^3, Z = 4, d_{calc} = 1.27 g/cm^3, μ = 0.484 mm^{-1}. A total of 6956 (5575 independent, R_{int} = 1.97%) reflections were collected at room temperature on a Siemens R3m/v diffractometer over a 2θ range of 3.5–45.0°. Of these 3595 were considered observed ($F > 4\sigma(F)$) and used in the refinements. Structure solution was by direct methods using SHELXTL. Full-matrix least-squares refinement of structural parameters (hydrogen as riding atoms) gave R = 0.0682 and R_w = 0.0822.
(6) Crystal data for II: $C_{29}H_{39}B_2F_3N_{12}O_9SV_2$, M = 912.3, orthorhombic, $P2_12_12_1$, a = 12.309(3) Å, b = 16.197(2) Å, c = 20.232 Å, V = 4033.9(9) Å^3, Z = 4, d_{calc} = 1.502 g/cm^3, μ = 0.593 mm^{-1}. A total of 3319 (3133 independent, R_{int} = 2.87%) reflections were collected at room temperature on a Siemens R3m/v diffractometer over a 2θ range of 3.5–43.0°. Structure solution was by direct methods using SHELXTL. Full-matrix least-squares refinement of structural parameters (hydrogen atoms riding) gave R = 0.0499 and R_w = 0.0509 for 2333 reflections (F>3.0σ(F)).

0020-1669/93/1332-3589$04.00/0

when it again rises sharply. This behavior is characteristic of an antiferromagnetically coupled dimer with an $S = 0$ ground state containing a small quantity of a paramagnetic impurity. A fit to the data using the Heisenberg–Dirac–Van Vleck model for $S_1 = 1 = S_2$ and $H = -2JS_1 \cdot S_2$ was excellent and gave values of $J = -31.3(2)$ cm^{-1}, $g = 2.01(1)$, and TIP = 0.007(1) and a 0.7(1)% paramagnetic impurity.

It is clear upon examination that all of the first row $[L_2M_2(\mu\text{-O})(\mu\text{-RCO}_2)_2]$ complexes have a M–O–M bond angle very near 120° which changes very little, if at all, upon protonation.[1] This suggests an essentially sp^2-hybridized bridging-oxygen atom in both forms. The remarkable feature of the V(III) dimer system is the large value of the bridging V–O–V angle in the μ-oxo dimers and its significant decrease upon protonation. We interpret this as indicating that the bridging oxygen in **I** is approaching sp hybridization, where π-bonding interactions between it and the very oxophilic vanadium would be maximized at an angle of 180°.[7] However, the angle is actually constrained to a smaller value by the "bite" of the cobridging carboxylates. That the V–O–V unit favors a linear geometry is supported by the observation that the $[L_2V_2(\mu\text{-O})(\mu\text{-RCO}_2)_2]$ complexes reported here are relatively unstable in solution and are easily converted to deep-violet, linear, oxo-bridged complexes by loss of the bridging carboxylates.[8] Norton and co-workers have recently found that protonation rates for metal oxo bridges are far slower than expected based on simple organic models.[9] These workers attribute this, at least partly, to a change in hybridization of the bridging oxygen upon protonation which provides a barrier to the reaction.

Finally with respect to the switchover in the magnetic exchange interaction upon protonation; a possible explanation for this behavior originates with a consideration of the ferromagnetic coupling observed in nearly all linear μ-oxo V(III) dimers.[10-12] Here the triplet ground state results from occupation of the doubly degenerate, non-bonding HOMO ($\Phi_\Gamma = (2)^{-1/2}(d_\Gamma^{(1)} - d_\Gamma^{(2)}$, $\Gamma = xz, yz$) by only two metal d electrons.[13,14] When the V–O–V bridge is bent, the degeneracy of the HOMO is lifted with one orbital becoming progressively more antibonding in energy while the other remains nonbonding. The crossover from FM to AFM coupling could then result from a combination of the effect of decreasing the bridge angle (caused by a change in hybridization of the oxygen upon protonation), which should favor increased AFM coupling, and increasing the V–O bond distance which should favor a decrease in the magnitude of the ferromagnetic coupling. Our research efforts are currently directed, through extended Huckel calculations and preparation of new V(III) dimers with a range of bridge angles, toward unraveling the role of these two geometrical parameters in the mechanism of the exchange crossover in this system.

Acknowledgment. This work was partially supported by Grant AI-1157 from the Robert A. Welch Foundation and Grant 3615-002 from the Texas Advanced Research Program to C.J.C. The authors also thank the NSF-ILI program through Grant USE-9151286 for support of the X-ray diffraction facilities at Southwest Texas State University.

Supplementary Material Available: Tables giving a structure determination summary, positional parameters, bond lengths and angles, anisotropic thermal parameters, and hydrogen atom parameters for **I** and **II** (21 pages). Ordering information is given on any current masthead page.

(7) Even V(III) is surprisingly oxophilic with V(III)–alkoxide bonds being very short and indicative of considerable π-bonding interaction. Carrano *et al.* Unpublished data.
(8) Carrano *et al.* unpublished observations.
(9) Carroll, J. M.; Norton, J. R. *J. Am. Chem. Soc.* **1992**, *114*, 8744.
(10) Brand, S. G.; Edelstein, N.; Hawkins, C. J.; Shalimoff, G.; Snow, M. R.; Tiekink, E. R. T. *Inorg. Chem.* **1990**, *29*, 434.
(11) Knopp, P.; Wieghardt, K.; Nuber, B.; Weiss, J.; Sheldrick, W. S. *Inorg. Chem.* **1990**, *29*, 363.
(12) Money, J. K.; Folting, K.; Huffman, J. C.; Christou, G. *Inorg. Chem.* **1987**, *26*, 944.
(13) Hay, J. P.; Thibeault, J. C.; Hoffman, R. *J. Am. Chem. Soc.* **1975**, *97*, 4884.
(14) Tatsumi, K.; Hoffman, R. *J. Am. Chem. Soc.* **1981**, *103*, 3328.